Scientia Iranica B (2015) 22(1), 196–207

SCIENTIA IRANICA

Sharif University of Technology
Scientia Iranica
Transactions B: Mechanical Engineering
www.scientiairanica.com

A finite element formulation for bending analysis of isotropic and orthotropic plates based on two-variable refined plate theory

J. Rouzegar* **and R. Abdoli Sharifpoor**

Department of Mechanical and Aerospace Engineering, Shiraz University of Technology, Shiraz, P.O. Box 71555-313, Iran.

Received 28 July 2013; received in revised form 10 March 2014; accepted 31 May 2014

KEYWORDS
Finite element method;
Two-variable plate theory;
Rectangular plate element;
Orthotropic plate.

Abstract. A finite element formulation based on two-variable refined plate theory has been developed in this paper and has been implemented for bending analysis of isotropic and orthotropic plates. The two-variable refined plate theory can be used for thin and thick plates and predicts parabolic variation of transverse shear stresses across the plate thickness. In this theory the zero traction condition on the plate surfaces is satisfied without using shear correction factor. The governing equations have been derived using the principle of minimum potential energy. After constructing weak form equations, a new 4-node rectangular plate element with six degrees of freedom at each node has been used for discretization of the domain. The finite element code is written in MATLAB and some benchmark problems have been solved. Comparison of results with exact solution and other common plate theories shows the accuracy and efficiency of presented finite element formulation.

1. Introduction

Classical Plate Theory (CPT) is the simplest plate theory that gives good results for bending analysis of thin plates but it does not take into account shear deformation effects [1]. The effect of shear deformation is important in bending analysis of thick plates and also for thin plates vibrating at higher modes; so numerous researchers have attempted to refine the CPT. Reissner proposed First order Shear Deformation Theory (FSDT) based on stress approach [2] and another form of FSDT was proposed by Mindlin [3] based on displacement approach. The FSDT predicts the constant transverse shear stress along the plate thickness, and, hence, the shear correction factor is required for satisfying the free stress conditions on the plate surfaces. To avoid the use of shear correction factor, the Higher-order Shear Deformation Theories (HSDTs) were developed. Second-order shear deformation theory of Whitney and Sun [4], third-order shear deformation theory of Hanna and Leissa [5], Reddy [6], Reddy and Phan [7], Bhimaraddi and Stevens [8], Kant [9] and Lo et al. [10] are the most famous HSDTs.

Recently, some new higher order shear deformation theories such as trigonometric shear deformation theory [11], hyperbolic shear deformation theory [12] and two-variable refined plate theory [13] have been developed. The two-variable plate theory is a simple and efficient theory that contains only two unknown variables which are bending and shear components of transverse displacement. This theory satisfies the condition of free stress at the plate surfaces without using shear correction factor. It was introduced by Shimpi [13] for isotropic plates and then extended to orthotropic plates by Shimpi and Patel [14] and Thai and Kim [15]. The analysis of laminated composite plates was done by Kim et al. [16] and the vibration

*. *Corresponding author. Tel./Fax: +98 711 7264102*
E-mail address: rouzegar@sutech.ac.ir (J. Rouzegar)

and buckling analysis of plates were performed by Shimpi and Patel [17] and Kim et al. [18], respectively. Analysis of free vibration of FGM plates rested on elastic foundation performed by Thai and Choi [19].

Previous researchers have adopted the two-variable plate theory and presented analytical solutions for some plate problems with specific geometry, loading and boundary conditions. In practice, it is too difficult to solve many engineering problems by common analytical methods. Using numerical approaches such as Finite Element Method (FEM), the complicated problems could be simulated in an approximate manner. Finite element analysis became quick, precise and popular by the advancements in computer science. Recently a new shear deformation plate finite element formulation was introduced by Patel and Shimpi [20]. They represent a C^1 continuity element with complete bicubic Hermite interpolation function. Katori and Okada [21] developed a finite element formulation based on refined plate theory using triangular and quadrilateral elements for discretization of the domain.

In this study a new finite element formulation based on two-variable refined plate theory has been developed for bending analysis of thin and thick orthotropic plates. A new 4-node rectangular plate element with six degrees of freedom at each node has been introduced. The developed formulation has been validated by some benchmark problems in the literature.

2. Two-variable plate theory

The two-variable refined plate theory is constructed based on following assumptions:

1. The in-plane displacements (u in x-direction, v in y-direction and w in z-direction) are negligible relative to the plate thickness. So the strain-displacement relations can be expressed as:

$$\begin{cases} \varepsilon_x = \frac{\partial u}{\partial x}, & \gamma_{xy} = \frac{\partial v}{\partial x} + \frac{\partial u}{\partial y}, \\ \varepsilon_y = \frac{\partial v}{\partial y}, & \gamma_{yz} = \frac{\partial w}{\partial y} + \frac{\partial v}{\partial z}, \\ \varepsilon_z = \frac{\partial w}{\partial z}, & \gamma_{zx} = \frac{\partial w}{\partial x} + \frac{\partial u}{\partial z}. \end{cases} \tag{1}$$

2. The transverse displacement w has two components: the bending and shear component (w_b and w_s):

$$w(x, y, t) = w_b(x, y, t) + w_s(x, y, t). \tag{2}$$

3. The stress normal to the middle plane, σ_z, is small compared with the other stress components and may be neglected in the stress-strain relations. Consequently, the stress-strain relations for an orthotropic plate can be written as:

$$\begin{cases} \sigma_x = \frac{E_1}{(1-\mu_{12}\mu_{21})}\varepsilon_x + \frac{\mu_{12}E_2}{(1-\mu_{12}\mu_{21})}\varepsilon_y, & \tau_{xy} = G_{12}\gamma_{xy}, \\ \sigma_y = \frac{E_2}{(1-\mu_{12}\mu_{21})}\varepsilon_y + \frac{\mu_{21}E_1}{(1-\mu_{12}\mu_{21})}\varepsilon_x, & \tau_{yz} = G_{23}\gamma_{yz}, \\ \sigma_z = 0, & \tau_{zx} = G_{31}\gamma_{zx}, \end{cases} \tag{3}$$

where E_1 and E_2 are elastic modulus, G_{12}, G_{23} and G_{31} are shear modulus, and μ_{12} and μ_{21} are Poisson's ratios.

4. The displacements in x and y directions consist of bending and shear components:

$$u = u_b + u_s, \qquad v = v_b + v_s. \tag{4}$$

The bending components of displacement play the same roles as u and v in classical plate theory. So we can write:

$$u_b = -z\frac{\partial w_b}{\partial x}, \qquad v_b = -z\frac{\partial w_b}{\partial y}. \tag{5}$$

Based on the above assumptions, the displacements can be calculated as:

$$u(x, y, z) = -z\frac{\partial w_b}{\partial x} + h\left[\frac{1}{4}\left(\frac{z}{h}\right) - \frac{5}{3}\left(\frac{z}{h}\right)^3\right]\frac{\partial w_s}{\partial x}, \tag{6}$$

$$v(x, y, z) = -z\frac{\partial w_b}{\partial y} + h\left[\frac{1}{4}\left(\frac{z}{h}\right) - \frac{5}{3}\left(\frac{z}{h}\right)^3\right]\frac{\partial w_s}{\partial y}, \tag{7}$$

$$w(x, y, t) = w_b(x, y, t) + w_s(x, y, t). \tag{8}$$

The strain field is obtained by substituting Eqs. (6)-(8) in Eq. (1):

$$\varepsilon_x = -z\frac{\partial^2 w_b}{\partial x^2} + h\left[\frac{1}{4}\left(\frac{z}{h}\right) - \frac{5}{3}\left(\frac{z}{h}\right)^3\right]\frac{\partial^2 w_s}{\partial x^2}, \tag{9}$$

$$\varepsilon_y = -z\frac{\partial^2 w_b}{\partial y^2} + h\left[\frac{1}{4}\left(\frac{z}{h}\right) - \frac{5}{3}\left(\frac{z}{h}\right)^3\right]\frac{\partial^2 w_s}{\partial y^2}, \tag{10}$$

$$\varepsilon_z = 0, \tag{11}$$

$$\gamma_{xy} = -2z\frac{\partial^2 w_b}{\partial x \partial y} + 2h\left[\frac{1}{4}\left(\frac{z}{h}\right) - \frac{5}{3}\left(\frac{z}{h}\right)^3\right]\frac{\partial^2 w_s}{\partial x \partial y}, \tag{12}$$

$$\gamma_{yz} = \left[\frac{5}{4} - 5\left(\frac{z}{h}\right)^2\right]\frac{\partial w_s}{\partial y}, \tag{13}$$

$$\gamma_{xz} = \left[\frac{5}{4} - 5\left(\frac{z}{h}\right)^2\right]\frac{\partial w_s}{\partial x}. \tag{14}$$

Substituting strains from Eqs. (9)-(14) in constitutive Eqs. (3), the expressions for stresses can be obtained as:

$$\begin{Bmatrix} \sigma_x \\ \sigma_y \\ \tau_{xy} \\ \tau_{yz} \\ \tau_{zx} \end{Bmatrix} = \begin{bmatrix} Q_{11} & Q_{12} & 0 & 0 & 0 \\ Q_{12} & Q_{22} & 0 & 0 & 0 \\ 0 & 0 & Q_{66} & 0 & 0 \\ 0 & 0 & 0 & Q_{44} & 0 \\ 0 & 0 & 0 & 0 & Q_{55} \end{bmatrix} \begin{Bmatrix} \varepsilon_x \\ \varepsilon_y \\ \gamma_{xy} \\ \gamma_{yz} \\ \gamma_{zx} \end{Bmatrix}, \tag{15}$$

where:

$$\begin{cases} Q_{11} = \frac{E_1}{1-\mu_{12}\mu_{21}}, \quad Q_{12} = \frac{\mu_{12}E_2}{1-\mu_{12}\mu_{21}} = \frac{\mu_{21}E_2}{1-\mu_{12}\mu_{21}}, \\ Q_{22} = \frac{E_2}{1-\mu_{12}\mu_{21}}, \\ Q_{44} = G_{23}, \qquad Q_{55} = G_{31}, \quad Q_{66} = G_{12}. \end{cases} \tag{16}$$

Using principle of minimum potential energy, the governing equations and boundary conditions will be obtained. Total potential energy of the plate can be written as:

$$U = \int_{z=-h/2}^{z=h/2} \int_{y=0}^{y=b} \int_{x=0}^{x=a} \frac{1}{2}[\sigma_x\varepsilon_x + \sigma_y\varepsilon_y + \tau_{xy}\gamma_{xy} + \tau_{yz}\gamma_{yz} + \tau_{zx}\gamma_{zx}]dxdydz + \int_0^a \int_0^b qwdxdy, \tag{17}$$

where q is the intensity of distributed load in z-direction. Substituting stress and strain fields into Eq. (17) and taking into account the independent variations of w_b and w_s, the governing equations can be obtained, as follows:

$$D_{11}\frac{\partial^4 w_b}{\partial x^4} + 2(D_{12}+2D_{66})\frac{\partial^4 w_b}{\partial x^2\partial y^2} + D_{22}\frac{\partial^4 w_b}{\partial y^4} = q, \tag{18}$$

$$\frac{1}{84}\left[D_{11}\frac{\partial^4 w_s}{\partial x^4} + 2(D_{12}+2D_{66})\frac{\partial^4 w_s}{\partial x^2\partial y^2} + D_{22}\frac{\partial^4 w_s}{\partial y^4}\right] - \left[A_{55}\frac{\partial^2 w_s}{\partial x^2} + A_{44}\frac{\partial^2 w_s}{\partial y^2}\right] = q, \tag{19}$$

where D_{11}, D_{22}, D_{12}, D_{66}, A_{44} and A_{55} are plate material stiffness, expressed by:

$$\begin{cases} D_{11} = \frac{Q_{11}h^3}{12}, \quad D_{22} = \frac{Q_{22}h^3}{12}, \quad D_{12} = \frac{Q_{12}h^3}{12}, \\ D_{66} = \frac{Q_{66}h^3}{12}, \\ A_{44} = \frac{5Q_{44}h}{6}, \quad A_{55} = \frac{5Q_{55}h}{6}. \end{cases} \tag{20}$$

As seen in Eqs. (18) and (19), the governing equations for bending of orthotropic plates consist of two uncoupled forth-order differential equations. Different possible boundary conditions are discussed in [14].

3. Finite element formulation

3.1. Weak form equations

For a plate element with volume v_e and mid-plane Ω_e, the principle of minimum potential energy can be written as:

$$\int_{v_e} \delta(\sigma_{xx}\varepsilon_{xx} + \sigma_{yy}\varepsilon_{yy} + \sigma_{xy}\gamma_{xy} + \sigma_{xz}\gamma_{xz} + \sigma_{yz}\gamma_{yz})dv$$

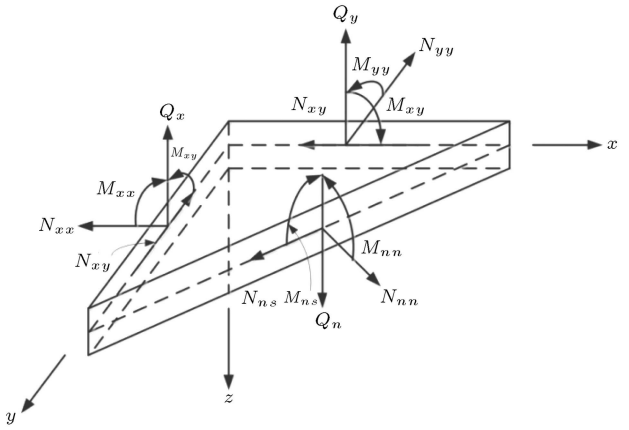

Figure 1. Bending moments and shear forces on a plate element.

$$-\int_{\Omega_e} q\delta w dxdy - \oint_{\Gamma_e}\left(-M_{nn}\frac{\partial\delta w}{\partial n} + V_n\delta w\right)ds = 0, \tag{21}$$

where M_{nn} and V_n denote the bending moment and effective shear force, respectively, as shown in Figure 1. The effective shear force can be defined as:

$$V_n = Q_n + \frac{\partial M_{ns}}{\partial s}. \tag{22}$$

Substituting the stress and strain fields into Eq. (21), we obtain:

$$\begin{aligned} \delta\pi = &\int_{\Omega_e} \begin{pmatrix} \left(D_{11}\frac{\partial^2 w_b}{\partial x^2} + D_{12}\frac{\partial^2 w_b}{\partial y^2}\right)\frac{\partial^2\delta w_b}{\partial x^2} \\ + \left(D_{12}\frac{\partial^2 w_b}{\partial x^2} + D_{22}\frac{\partial^2 w_b}{\partial y^2}\right)\frac{\partial^2\delta w_b}{\partial y^2} \\ +4D_{66}\frac{\partial^2 w_b}{\partial x\partial y}\frac{\partial^2\delta w_b}{\partial x\partial y} \end{pmatrix} dxdy \\ &+\int_{\Omega_e}\left(\frac{1}{84}\begin{pmatrix} \left(D_{11}\frac{\partial^2 w_s}{\partial x^2} + D_{12}\frac{\partial^2 w_s}{\partial y^2}\right)\frac{\partial^2\delta w_s}{\partial x^2} \\ + \left(D_{12}\frac{\partial^2 w_s}{\partial x^2} + D_{22}\frac{\partial^2 w_s}{\partial y^2}\right)\frac{\partial^2\delta w_s}{\partial y^2} \\ +4D_{66}\frac{\partial^2 w_s}{\partial x\partial y}\frac{\partial^2\delta w_s}{\partial x\partial y} \end{pmatrix}\right. \\ &\left. + \left(A_{44}\frac{\partial w_s}{\partial x}\frac{\partial\delta w_s}{\partial x} + A_{55}\frac{\partial w_s}{\partial y}\frac{\partial\delta w_s}{\partial y}\right)\right)dxdy \\ &-\int_{\Omega_e} q\delta(w_b + w_s)dxdy \\ &+\oint_{\Gamma_e}\left(-M_{nn}\frac{\partial\delta(w_b+w_s)}{\partial n} + V_n\delta(w_b+w_s)\right)ds. \end{aligned} \tag{23}$$

Equating variation of potential energy to zero, the weak form of governing equations is found as:

$$\int_{\Omega^e}\Bigg[\left((D_2\delta w_b)^T D(D_2 w_b)\right)+\left(\frac{1}{84}(D_2\delta w_s)^T D(D_2 w_s)+(D_1\delta w_s)^T A(D_1 w_s)\right)\Bigg]dxdy-\int_{\Omega^e}\left[\delta(w_b+w_s)^T q\right]dxdy-\oint_{\Gamma_e}\Bigg[-\left(\frac{\delta(\partial(w_b+w_s)}{\partial n}\right)^T M_{nn}+\left(\delta(w_b+w_s)\right)^T V_n\Bigg]ds=0, \tag{24}$$

where A, D, D_1 and D_2 are defined as:

$$A=\begin{bmatrix}A_{44} & 0\\ 0 & A_{55}\end{bmatrix},\qquad D=\begin{bmatrix}D_{11} & D_{12} & 0\\ D_{12} & D_{22} & 0\\ 0 & 0 & D_{66}\end{bmatrix},$$

$$D_1=\begin{Bmatrix}\frac{\partial}{\partial x}\\ \\ \frac{\partial}{\partial y}\end{Bmatrix},\qquad D_2=\begin{Bmatrix}\frac{\partial^2}{\partial x^2}\\ \\ \frac{\partial^2}{\partial y^2}\\ \\ 2\frac{\partial^2}{\partial x\partial y}\end{Bmatrix}. \tag{25}$$

3.2. Discretized equations

The bending and shear transverse displacement fields can be determined by interpolating the nodal Degrees Of Freedom (DOFs) over the elements domain:

$$w_b(x,y)=\sum_{j=1}^{n}\Delta_j^b\varphi_j(x,y)=N^T\Delta_b,$$

$$w_s(x,y)=\sum_{j=1}^{n}\Delta_j^s\varphi_j(x,y)=N^T\Delta_s, \tag{26}$$

where Δ_b and Δ_s are bending and shear DOF vectors in each element, φ_j and N are interpolation functions and shape functions, respectively. Substituting Eq. (26) in Eq. (24), the finite element equations based on two-variable refined plate theory are obtained as:

$$\begin{bmatrix}K^{11} & 0\\ 0 & K^{22}\end{bmatrix}\begin{Bmatrix}\Delta_b\\ \Delta_s\end{Bmatrix}=\begin{Bmatrix}F\\ F\end{Bmatrix}, \tag{27}$$

where:

$$K^{11}=\int_{\Omega_e}(B_2^T D B_2)dxdy, \tag{28}$$

$$K^{22}=\int_{\Omega_e}\left(\frac{1}{84}B_2^T D B_2+B_1^T A B_1\right)dxdy, \tag{29}$$

$$F=\int_{\Omega_e}Nqdxdy-\oint_{\Gamma_e}\left(\frac{\partial N}{\partial n}M_{nn}+\frac{\partial N}{\partial s}M_{ns}+NQ_n\right), \tag{30}$$

where B_1 and B_2 are:

$$B_1=D_1N,\qquad B_2=D_2N. \tag{31}$$

If the effect of shear deformation is ignored and just bending degrees of freedom, Δ_b, are considered, the finite element formulation for classical plate theory will be obtained as

$$[K^{11}]\{\Delta_b\}=\{F\}. \tag{32}$$

This formulation was presented by many researchers in the literature [22].

3.3. Element design

According to Eq. (24), bending and shear components of transverse displacements and their normal derivatives can be chosen as the primary variables. Because $\partial/\partial n$ is related to global derivatives $\partial/\partial x$ and $\partial/\partial y$, the degree of freedoms will be:

$$\text{DOFs}:\left\{w_b\quad \frac{\partial w_b}{\partial x}\quad \frac{\partial w_b}{\partial y}\quad w_s\quad \frac{\partial w_s}{\partial x}\quad \frac{\partial w_s}{\partial y}\right\}. \tag{33}$$

In order to complete the development of finite element formulation of two-variable plate theory, an element including bending and shear properties is required. For this purpose a 4-node rectangular plate element with six degrees of freedom at each node is introduced. Regarding Eq. (26), the elemental bending and shear DOFs will be:

$$\left(\Delta^b\right)^T=\left[w_1^b\quad \left(\frac{\partial w_b}{\partial y}\right)_1\quad \left(-\frac{\partial w_b}{\partial x}\right)_1\quad\cdots\quad \left(-\frac{\partial w_b}{\partial x}\right)_4\right],$$

$$\left(\Delta^s\right)^T=\left[w_1^s\quad \left(\frac{\partial w_s}{\partial y}\right)_1\quad \left(-\frac{\partial w_s}{\partial x}\right)_1\quad\cdots\quad \left(-\frac{\partial w_s}{\partial x}\right)_4\right]. \tag{34}$$

Thus each element has 24 degrees of freedom. If the shear and bending nodal DOFs are defined as a_i^b and a_i^s, respectively, and the elemental shear and bending DOFs are defined as a_e^b and a_e^s, we will have:

$$a_e^b=\begin{Bmatrix}a_i^b\\ a_j^b\\ a_k^b\\ a_l^b\end{Bmatrix},\qquad a_i^b=\begin{Bmatrix}w_b\\ \partial w_b/\partial y\\ -\partial w_b/\partial x\end{Bmatrix},$$

$$a_e^s=\begin{Bmatrix}a_i^s\\ a_j^s\\ a_k^s\\ a_l^s\end{Bmatrix},\qquad a_i^s=\begin{Bmatrix}w_s\\ \partial w_s/\partial y\\ -\partial w_s/\partial x\end{Bmatrix}. \tag{35}$$

The shape functions used in this study had been derived by Melosh [23]. According to shear and bending

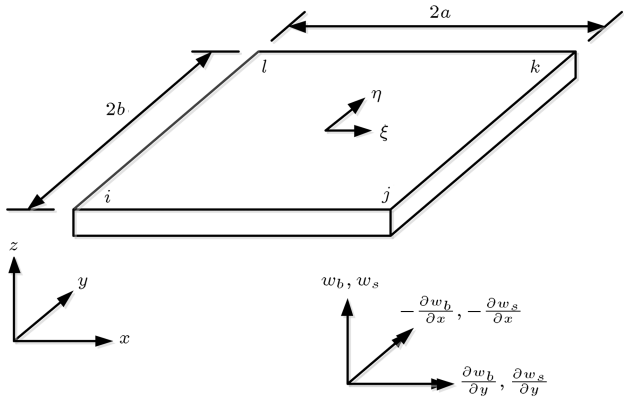

Figure 2. Rectangular plate element.

nodal DOFs, a_i^b and a_i^s, the shape functions in terms of normalized coordinates are defined as:

$$N_i^T = \frac{1}{8}(1+\xi_0)(1+\eta_0)\begin{Bmatrix}(2+\xi_0+\eta_0-\xi^2-\eta^2)\\ b\eta_i(1-\eta^2)\\ -a\xi_i(1-\xi^2)\end{Bmatrix},$$

$$\xi = (x-x_c)/a, \qquad \eta = (y-y_c)/b, \qquad \xi_0 = \xi\xi_i,$$

$$\eta_0 = \eta\eta_i, \tag{36}$$

where $2a$ and $2b$ are the width and length of rectangular element as shown in Figure 2.

4. Results and discussion

A FE code based on presented formulation is generated using MATLAB software. Some benchmark problems are solved by the code and the obtained results are compared with exact values and analytical solutions.

Example 1. A Simply supported isotropic square plate (of length and width, a, and thickness, h) subjected to uniformly distributed transverse load, q_0, is considered. This problem is simulated by presented finite element code based on two-variable refined plate theory (in short FE-RPT) considering different number of elements in mesh structure. The effect of number of elements on obtained normalized deflection of center of the plate ($x = a/2$, $y = b/2$) is shown in Figure 3. By increasing number of elements, obtained results converge to the value having 0.2% relative error with respect to exact solution. Using 16 elements in each plate side, the normalized transverse deflection, normal and shear stresses are obtained for various thicknesses to side ratio. The results are compared with some analytical solutions of common plate theories in Table 1. It is seen that the results of presented formulation are in good agreement with the exact values and other plate theories. The differences between CPT results and exact values are increased by increasing the thickness to side ratio because of ignoring the shear deformation effect in this theory; but the presented formulation has excellent capability in simulation of both thin and thick plates.

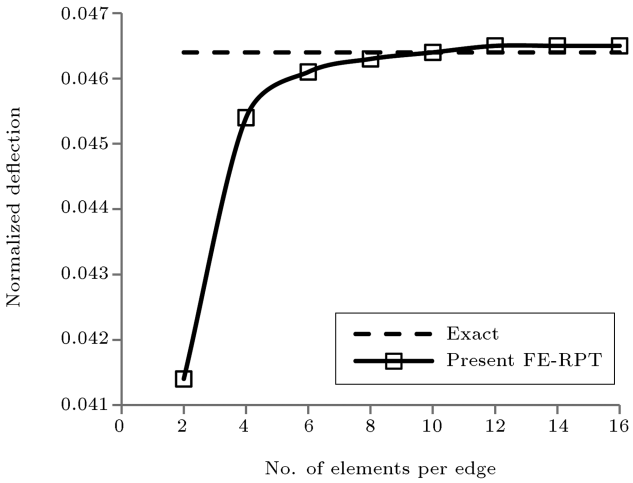

Figure 3. Convergence study for isotropic square plate subjected to uniform loading ($h/a = 0.1$).

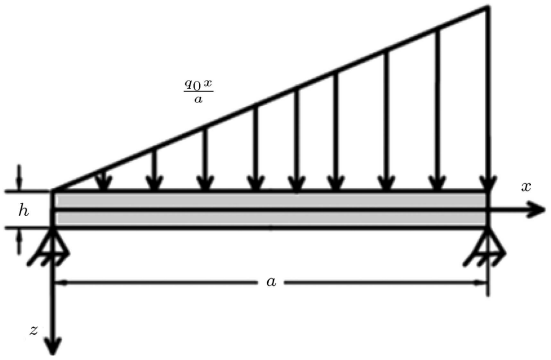

Figure 4. Simply supported rectangular plate subjected to linearly distributed load.

Example 2. A Simply supported isotropic square plate (of length and width, a, and thickness, h) subjected to linearly distributed load, as shown in Figure 4, is considered. As illustrated in Figure 5, by increasing number of elements, the normalized deflections converge to the value having 0.4% relative error with respect to exact solution. In Table 2, the transverse deflections and normal and shear stresses are compared with the exact values, analytical solutions of two-variable theory and other common theories. The obtained deflections and normal stresses are very close to exact values and other plate theories. Though the shear stresses obtained by FE-RPT are in good agreement with analytical solutions of two-variable plate theory, both FE-RPT and Analytical-RPT present lower shear stresses with respect to other theories.

Table 1. Comparison of deflections and stresses for a simply supported isotropic square plate subjected to uniformly distributed load.

h/a	Source	$\bar{w}^*$ $x=a/2,\ y=b/2$	$\bar{\sigma_x}^*$ $x=a/2,\ y=b/2,\ z=h/2$	$\bar{\tau_{xy}}^*$ $x=0, y=0,\ z=h/2$	$\bar{\tau_{xz}}^*$ $x=0,\ y=b/2,\ z=0$
0.2	FE-RPT	0.0535	0.2939	0.2083	0.4695
	HSDT [24]	0.0535	0.2944	0.2112	0.4840
	FSDT [24]	0.0536	0.2873	0.1946	0.3928
	CPT [24]	0.0444	0.2873	0.1946	0.0000
0.1	FE-RPT	0.0465	0.2883	0.1971	0.4718
	HSDT [24]	0.0467	0.2890	0.1990	0.4890
	FSDT [24]	0.0467	0.2873	0.1946	0.3928
	CPT [24]	0.0444	0.2873	0.1946	0.0000
	EXACT [24]	0.0464	—	—	—
0.05	FE-RPT	0.0449	0.2869	0.1941	0.4715
	CPT [24]	0.0444	0.2873	0.1946	0.0000
	EXACT [24]	0.0449	—	—	—
0.01	FE-RPT	0.0443	0.2865	0.1931	0.4702
	HSDT [24]	0.0444	0.2873	0.1947	0.4909
	FSDT [24]	0.0444	0.2873	0.1946	0.3928
	CPT	0.0444	0.2873	0.1946	0.0000

* $\bar{w} = \frac{Eh^3}{q_0 a^4} w$, $(\bar{\sigma}_x, \bar{\tau}_{xy}) = \frac{(\sigma_x, \tau_{xy})h^2}{q_0 a^2}$, $(\bar{\tau}_{xz}) = \frac{(\tau_{xz})h}{q_0 a}$.

Table 2. Comparison of deflections and stresses for a simply supported isotropic square plate subjected to linearly distributed load ($h/a = 0.1$).

Theory	$\bar{w}^*$ $x=a/2,\ y=b/2$	$\bar{\sigma_x}^*$ $x=a/2,\ y=b/2,\ z=h/2$	$\bar{\tau_{xy}}^*$ $x=0,\ y=0,\ z=h/2$	$\bar{\tau_{xz}}^*$ $x=0,\ y=b/2,\ z=0$
Present FE-RPT	2.3301	0.1442	0.0781	0.1345
Analytical-RPT	2.3329	0.1445	0.0873	0.1348
TSDT [11]	2.3125	0.1535	0.0975	0.2522
HSDT [6]	2.3325	0.1445	0.0995	0.2463
FSDT [3]	2.3350	0.1435	0.0975	0.1650
CPT [1]	2.2180	0.1435	0.0975	0.0000
EXACT [25]	2.3195	0.1445	—	—

* $\bar{w} = \frac{Eh^3}{q_0 a^4} w$, $(\bar{\sigma}_x, \bar{\tau}_{xy}) = \frac{(\sigma_x, \tau_{xy})h^2}{q_0 a^2}$, $(\bar{\tau}_{xz}) = \frac{(\tau_{xz})h}{q_0 a}$.

Table 3. Material properties of orthotropic plate.

E_2/E_1	G_{12}/E_1	G_{13}/E_1	G_{23}/E_1	μ_{12}	μ_{21}
0.525	0.26293	0.15991	0.26293	0.44026	0.23124

Example 3. A simply supported orthotropic rectangular plate with material properties listed in Table 3 is subjected to a uniformly distributed transverse load, q_0. Considering different mesh designs, the problem is simulated by presented FE-RPT code, and the obtained transverse deflections and in-plane stresses are listed in Table 4. As it is observed, by increasing number of elements, the results converge to values which are in good agreement with exact solutions.

As discussed in Eq. (32), the CPT formulation is achieved by neglecting the shear component of transverse deflection. Results for central transverse deflection of the plate, obtained by FE-CPT and FE-RPT formulations, are compared with the exact values in Figure 6. As illustrated in this figure, in comparison to FE-CPT formulation, the normalized transverse deflections extracted from FE-RPT formulation are more accurate. By increasing number of elements, FE-RPT deflections converge to the value with only 1.6% relative error respect to exact solution,

Table 4. Normalized transverse deflections and in-plane normal stresses for simply supported orthotropic rectangular plate subjected to uniformly distributed loading ($a/b = 0.5$, $h/a = 0.1$).

Method	Mesh design	$\bar{w}^*$ $x = a/2,\ y = b/2$	$\bar{\sigma_x}^*$ $x = a/2,\ y = b/2,\ z = h/2$	$\bar{\sigma_y}^*$ $x = a/2,\ y = b/2,\ z = h/2$
Present FE-RPT	2×4	1241.8	66.610	18.327
Present FE-RPT	4×8	1387.6	64.496	19.199
Present FE-RPT	6×12	1413.3	66.051	19.767
Present FE-RPT	8×16	1422.6	66.564	19.958
Present FE-RPT	10×20	1427.1	66.828	20.058
Present FE-RPT	12×24	1429.6	66.981	20.116
Present FE-RPT	14×28	1431.1	67.075	20.152
Present FE-RPT	16×32	1432.0	67.137	20.175
EXACT [15]	—	1408.5	65.975	20.204

* $\bar{w} = wQ_{11}/hq_0$, $(\bar{\sigma}_x, \bar{\sigma}_y, \bar{\tau}_{xy}) = \frac{(\sigma_x, \sigma_y, \tau_{xy})}{q_0}$.

Table 5. Comparison of Normalized transverse deflection for simply supported orthotropic plate.

Plate parameters		$\bar{w}^*(x = a/2, y = b/2)$		
a/b	h/a	EXACT [14]	Analytical-RPT [14]	FE-RPT
0.5	0.05	21542	21513	21889
	0.1	1408.5	1402.2	1432.0
	0.14	387.23	384.2	393.81
1	0.05	10443	10413	10802
	0.1	688.57	688.37	709.44
	0.14	191.07	191.02	196.09
2	0.05	2048.7	2047.9	2098.4
	0.1	139.08	138.93	142.4
	0.14	39.79	39.75	40.81

* $\bar{w} = wQ_{11}/hq_0$

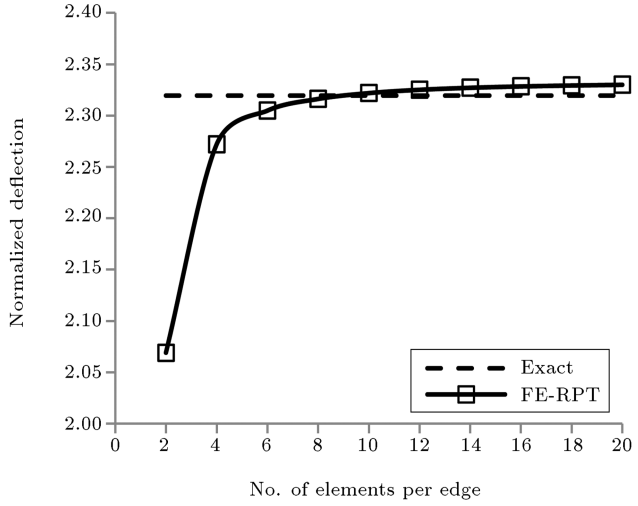

Figure 5. Convergence study for isotropic square plate subjected to linear loading ($h/a = 0.1$).

whereas this error for FE-CPT formulation is about 4.4%.

In Tables 5-8 normalized transverse deflections and normal and shear stresses obtained by FE-RPT code are compared with the exact values and the results obtained by analytical solution of two-variable plate theory. As it is seen, the presented formulation has good capability in estimation of these parameters. Also the effects of aspect ratio (a/b) and thickness to side ratio (h/a) on the results are investigated and it is seen that the differences between FE-RPT results and exact values are increased by increasing the aspect ratio. The normalized transverse shear stresses $\bar{\tau}_{xz}$ for different values of (a/b) and (h/a) are listed in Table 8. It is observed that the stresses obtained by FE-RPT are in good agreement with analytical solution of two-variable plate theory but have considerable differences with respect to exact value. In the other word, both

Table 6. Comparison of normalized in-plane normal stress $\bar{\sigma}_x$ for simply supported orthotropic plate.

Plate parameters		$\bar{\sigma_x}^*(x=a/2, y=b/2, z=h/2)$		
a/b	h/a	EXACT [14]	Analytical-RPT [14]	FE-RPT
0.5	0.05	262.67	262.78	266.86
	0.1	65.97	66.07	67.07
	0.14	33.86	33.96	34.49
1	0.05	144.31	144.68	149.90
	0.1	36.02	36.36	37.67
	0.14	18.34	18.68	19.37
2	0.05	40.65	40.98	41.85
	0.1	10.02	10.33	10.55
	0.14	5.03	5.32	5.41

* $\bar{\sigma}_x = \sigma_x/q_0$

Table 7. Comparison of normalized in-plane normal stress $\bar{\sigma}_y$ for simply supported orthotropic plate.

Plate parameters		$\bar{\sigma_y}^*(x=a/2, y=b/2, z=h/2)$		
a/b	h/a	EXACT [14]	Analytical-RPT [14]	FE-RPT
0.5	0.05	79.54	79.30	80.18
	0.1	20.20	19.94	20.15
	0.14	10.51	10.25	10.36
1	0.05	87.08	86.68	89.84
	0.1	22.21	21.80	22.61
	0.14	11.61	11.21	11.63
2	0.05	54.27	54.04	55.36
	0.1	13.88	13.65	14.00
	0.14	7.27	7.06	7.25

* $\bar{\sigma}_y = \sigma_y/q_0$

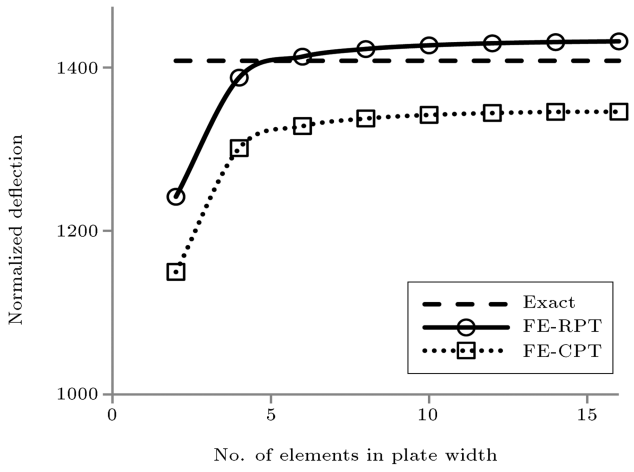

Figure 6. Convergence study of normalized transverse deflection of orthotropic rectangular plate obtained by FE-RPT and FE-CPT codes ($a/b = 0.5$, $h/a = 0.1$).

finite element modeling and analytical solution of two-variable plate theory give rise to lower transverse shear stresses with respect to exact values. This issue is related to the features of two-variable plate theory and was reported by previous researchers [14].

In Figures 7 and 8, the in-plane normal stresses are plotted across thickness of orthotropic plate for $h/a = 0.05$ and $h/a = 0.1$. These figures show that the in-plane normal stresses obtained by present FE formulation are in good agreement with the analytical solution and the exact values. Also the transverse shear stress is plotted in Figure 9 and as expected it varies parabolically across thickness of the plate. As previously mentioned, the transverse shear stresses obtained by both FE and analytical solution of two-variable plate theory have noticeable differences with respect to exact solution of orthotropic plate.

The most important challenge of plate theories is how to deal with transverse shear deformation effects. Because of different assumption adopted in common plate theories, the results of shear stresses for all theories have noticeable differences with each other and exact values. For example, as seen in Table 1, the shear stresses of isotropic plates predicted with different plate theories have differences with each other. In comparison to conventional higher order plate theories, the main feature of two-variable plate theory is its simplicity. This theory contains only two unknown parameters and it was adopted in various analyses such as

Table 8. Comparison of normalized transverse shear stress $\bar{\tau}_{xz}$ for simply supported orthotropic plate.

Plate parameters		$\bar{\tau}_{xz}^{*}(x=0, y=b/2, z=0)$		
a/b	h/a	EXACT [14]	Analytical-RPT [14]	FE-RPT
0.5	0.05	14.04	12.67	12.01
	0.1	6.92	6.31	6.01
	0.14	4.87	4.47	4.25
1	0.05	10.87	8.04	7.62
	0.1	5.34	4.02	3.80
	0.14	3.73	2.84	2.71
2	0.05	6.24	4.15	3.75
	0.1	2.95	2.03	1.86
	0.14	1.99	1.41	1.31

* $\bar{\tau}_{xz} = \tau_{xz}/q_0$

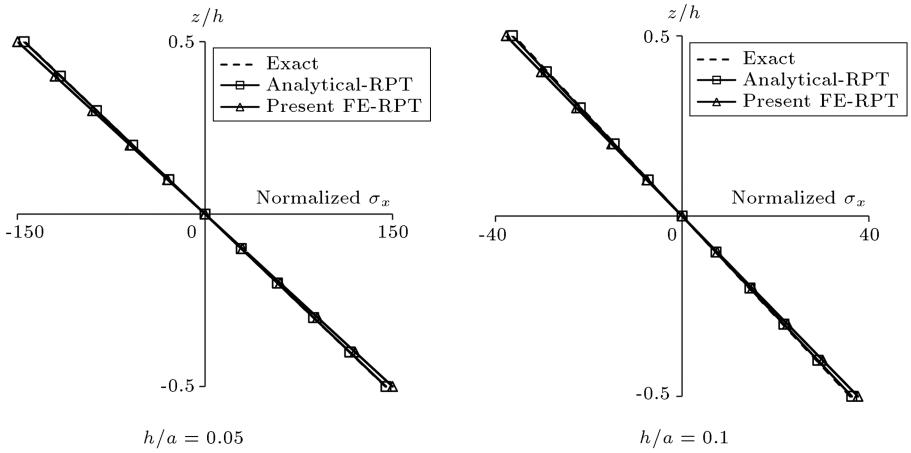

Figure 7. The variation of $\bar{\sigma}_x$ across thickness of orthotropic square plate.

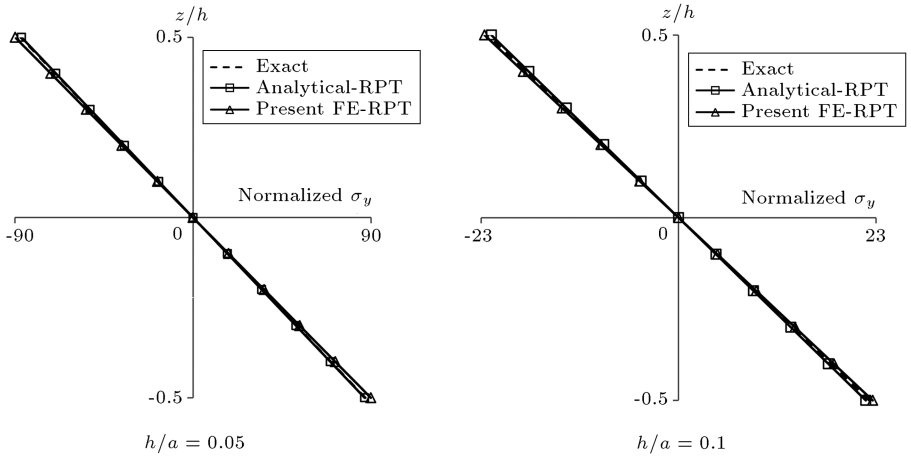

Figure 8. The variation of $\bar{\sigma}_y$ across thickness of orthotropic square plate.

bending, vibration and buckling problem easily [13-19]. For achieving a simpler and more efficient formulation, it is logical to lose some precision.

Parametric study. In this section, a parametric study on simply supported and fully clamped orthotropic square plates considering various aspect ratios has been performed and the obtained normalized transverse deflections, in-plane normal stresses and transverse shear stresses at the plate center are listed in Tables 9 and 10. The material properties except E_1/E_2 are chosen according to Table 3. As seen for both simply supported and clamped plates, by increasing E_1/E_2 ratio, the normalized transverse deflection and

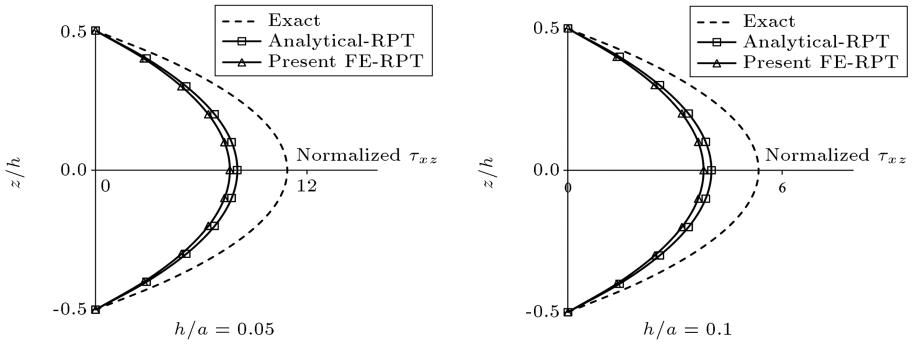

Figure 9. The variation of $\bar{\tau}_{xz}$ across thickness of orthotropic square plate.

Table 9. Normalized transverse deflections and in-plane normal stresses at the plate center for simply supported orthotropic square plates.

h/a	E_1/E_2	$\bar{w}$	$\bar{\sigma}_x$	$\bar{\sigma}_y$	$\bar{\tau}_{xz}$
0.05	1	8334.9	133.39	133.43	7.44
	2	10966	150.77	86.65	7.44
	4	12989	164.20	49.79	7.44
	5	13475	167.43	40.79	7.44
	8	14253	172.59	20.17	7.45
	10	14522	174.37	21.03	7.45
0.1	1	555.20	33.61	33.64	3.72
	2	719.61	37.91	21.80	3.72
	4	846.10	41.24	12.51	3.72
	5	876.46	42.04	10.25	3.72
	8	925.08	43.33	6.58	3.72
	10	941.89	43.77	5.28	3.72

Table 10. Normalized transverse deflections and in-plane normal stresses at the plate center fully clamped orthotropic square plates.

h/a	E_1/E_2	$\bar{w}$	$\bar{\sigma}_x$	$\bar{\sigma}_y$	$\bar{\tau}_{xz}$
0.05	1	2682.8	63.038	63.07	6.19
	2	3491.7	72.34	39.81	6.19
	4	4094.5	79.56	21.52	6.19
	5	4232.9	81.30	17.10	6.19
	8	4444.3	84.08	10.30	6.19
	10	4512.8	85.05	8.00	6.19
0.1	1	200.85	16.02	16.05	2.51
	2	251.61	18.30	10.09	2.52
	4	289.43	20.08	5.44	2.53
	5	298.12	20.51	4.34	2.53
	8	311.40	21.20	2.61	2.53
	10	315.72	21.44	2.03	2.53

stress $\bar{\sigma}_x$ are increased and the normalized stress $\bar{\sigma}_y$ is decreased; but the normalized out of plane shear stress $\bar{\tau}_{xz}$ is almost independent of E_1/E_2. As expected, the obtained deflections and stresses of simply supported plates are higher than clamed plates. This issue

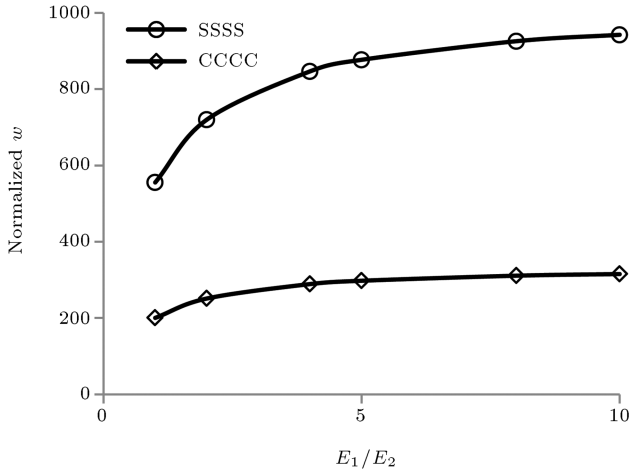

Figure 10. Comparison of normalized central deflection obtained for simply supported and fully clamped orthotropic square plate ($h/a = 0.1$).

is illustrated in Figures 10 and 11 for normalized deflection $\bar{w}$ and stress $\bar{\sigma}_x$, respectively.

5. Conclusion

In this study, a finite element formulation based on two-variable refined plate theory is developed. Unlike Classical Plate Theory (CPT), the presented formulation can be used for both thin and thick plates and predicts parabolic variation of transverse shear stresses across the plate thickness. Presented finite element formulation is free from shear locking and zero traction condition on the plate surfaces is satisfied without using shear correction factor. After constructing weak form equations using the principle of minimum potential energy, a new 4-node rectangular plate element with six degrees of freedom at each node has been introduced for discretization of the domains. The efficiency and accuracy of the presented formulation has been proved by solving of some benchmark isotropic and orthotropic plate problems. The obtained results are in good agreement with exact values and analytical solutions of common plate theories. The convergence of obtained results is confirmed by increasing the number

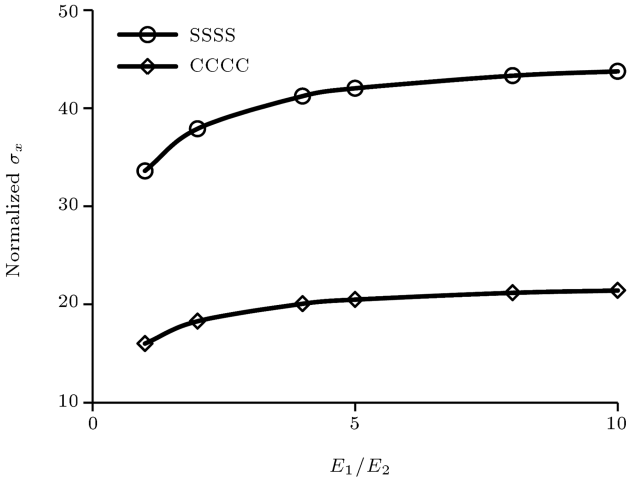

Figure 11. Comparison of normalized central stress $\bar{\sigma}_x$ obtained for simply supported and fully clamped orthotropic square plate ($h/a = 0.1$).

of elements in mesh design. Also the effects of aspect ratio, thickness to side ratio, material properties and type of boundary conditions on obtained results are investigated. Consequently, using presented finite element formulation, the thin and thick, and isotropic and orthotropic plate problems with arbitrary geometries and loadings can be simulated.

References

1. Kirchhoff, G. " Equilibrium and motion of an elastic disc" [Ä Über das gleichgewicht und die bewegung einer elastischen scheibe], *J. ReineAngew. Math.*, **1859**(40), pp. 51-88 (1850).
2. Reissner, E. "The effect of transverse shear deformation on the bending of elastic plates", *J. Appl. Mech.*, **12**(2), pp. 69-77 (1945).
3. Mindlin, R.D. "Influence of rotary inertia and shear on flexural motions of isotropic elastic plates", *J. Appl. Mech.*, **18**(1), pp. 31-8 (1951).
4. Whitney, J.M. and Sun, C.T. "A higher order theory for extensional motion of laminated composites", *J. Sound Vib.*, **30**(1), pp. 85-97 (1973).
5. Hanna, N.F. and Leissa, A.W. "A higher order shear deformation theory for the vibration of thick plates", *J. Sound Vib.*, **170**(4), pp. 545-555 (1994).
6. Reddy, J.N. "A simple higher-order theory for laminated composite plates", *ASME. J. Appl. Mech.*, **51**(4), pp. 745-752 (1984).
7. Reddy, J.N. and Phan, N.D. "Stability and vibration of isotropic, orthotropic and laminated plates according to a higher-order shear deformation theory", *J. Sound Vib.*, **98**(2), pp. 157-170 (1985).
8. Bhimaraddi, A. and Stevens, L.K. "A higher order theory for free vibration of orthotropic, homogeneous, and laminated rectangular plates", *J. Appl. Mech.*, **51**(1), pp. 195-198 (1984).
9. Kant, T. "Numerical analysis of thick plates", *Comput. Methods Appl. Mech. Eng.*, **31**(1), pp. 1-18 (1982).
10. Lo, K.H., Christensen, R.M. and Wu, E.M. "A high-order theory of plate deformation, Part 1: Homogeneous plates", *J. Appl. Mech.*, **44**(4), pp. 663-668 (1977).
11. Ghugal, Y.M. and Sayyad, A.S. "A static flexure of thick isotropic plates using trigonometric shear deformation theory", *J. Solid. Mech.*, **2**(1), pp. 79-90 (2010).
12. El Meiche, N., Tounsi, A., Ziane, N., Mechab, I. and Adda Bedia, E.A. "A new hyperbolic shear deformation theory for buckling and vibration of functionally graded sandwich plate", *Int. J. Mech. Sci.*, **53**(4), pp. 237-47 (2011).
13. Shimpi, R.P. "Refined plate theory and its variants", *AIAA J.*, **40**(1), pp. 137-146 (2002).
14. Shimpi, R.P. and Patel H.G. "A two variable refined plate theory for orthotropic plate analysis", *Int. J. Solids Struct.*, **43**(22), pp. 6783-6799 (2006).
15. Thai, H.T. and Kim, S.E. "Analytical solution of a two variable refined plate theory for bending analysis of orthotropic Levy-type plates", *Int. J. Mech. Sci.*, **54**(1), pp. 269-276 (2012).
16. Kim, S.E., Thai, H.T. and Lee, J. "A two variable refined plate theory for laminated composite plates", *J. Compos. Struct.*, **89**(2), pp. 197-205 (2009).
17. Shimpi, R.P. and Patel, H.G. "Free vibrations of plate using two variable refined plate theory", *J. Sound Vib.*, **296**(4-5), pp. 979-999 (2006).
18. Kim, S.E., Thai, H.T. and Lee, J. "Buckling analysis of plates using the two variable refined plate theory", *Thin Wall. Struct.*, **47**(4), pp. 455-462 (2009).
19. Thai, H.T. and Choi, D.H. "A refined shear deformation theory for free vibration of functionally graded plates on elastic foundation", *J. Compos. Eng.*, **43**(5), pp. 2335-2347 (2012).
20. Patel, H. and Shimpi, R.P. "A new finite element for a shear deformable plate", *47th AIAA/ASME/ASCE/AHS/ASC Structures, Structural Dynamics, and Materials Conf.*, Newport, Rhode Island, USA (2006).
21. Katori, H. and Okada, T. "Plate element based on a higher-order shear deformation theory", *Transactions of the Japan Society of Mechanical Engineers Series A*, **72**(716), pp. 412-418 (2006).
22. Reddy, J.N., *An Introduction to Finite Element Method*, 3rd Edn., McGraw-Hill International edition, Texas (2006).
23. Melosh, R.J. "Structural analysis of solids", *J. Struct. Div. ASCE*, **89**(4), pp. 205-223 (1963).
24. George, Z. and Robert, W. "Isotropic plate elements

with shear and normal strain deformations", *Int. J. Numer. Meth. Eng.*, **24**(9), pp. 1971-1695 (1987).

25. Srinivas, S., Joga C.V. and Rao, A.K. "Bending, vibration and buckling of simply supported thick orthotropic rectangular plate and laminates", *Int. J. Solids Struct.*, **6**(11), pp. 1463-1481 (1970).

Biographies

Seyyed Jafar Rouzegar is currently an assistant professor at the Department of Mechanical and Aerospace Engineering of Shiraz University of Technology, Iran. He received his BSc in Mechanical Engineering from Shiraz University, Iran, in 2002. He also received his MSc and PhD in Mechanical Engineering from Tarbiat Modares University, Iran, in 2004 and 2010, respectively. His research interests include: FEM and XFEM, Fracture Mechanics and Theories of Plates and Shells.

Reza Abdoli Sharifpoor received his BSc in Mechanical Engineering from Bu Ali Sina University, Hamedan, Iran, in 2011. He also received his MSc in Mechanical Engineering from Shiraz University of Technology, Iran, in 2014. His research interests include: FEM, theories of plates and shells and composite materials.